RESEARCH ARTICLE   OPEN ACCESS

Free Vibration Characteristics of Edge Cracked Piles with Circular Cross-Section

Dr. Şeref Doğuşcan Akbaş*
*(Civil Engineer, Şehit Muhtar Mah. Öğüt Sok. No:2/37 Beyoğlu/Istanbul, Turkey)

ABSTRACT
This paper focuses on free vibration analysis of an edge cracked pile with circular cross section. The soil medium is modelled as Winkler-Pasternak elastic foundation approach. The governing differential equations of motion are obtained by using Hamilton's principle. The pile–soil system is modeled as Euler–Bernoulli beam resting on Winkler-Pasternak foundation. The considered problem is solved by using finite element method. The cracked pile is modelled as an assembly of two sub-beams connected through a massless elastic rotational spring. In the study, the effects of the location of crack, the depth of the crack and the soil stiffness on the natural frequencies and mode shapes the piles are investigated in detail.
Keywords - Crack, Piles, Winkler-Pasternak Foundation, Free vibration, Finite element method

I.   INTRODUCTION

Piles are a type of deep soil foundation that commonly used in the civil engineering. The purpose of piles is to transmit the loads of a superstructure to the underlying soil, when the strength of soil base is insufficient to support the load from the superstructures. Piles are also used in the construction of offshore platforms, marine application and other structures that are situated over water.

Piles are not subjected to only gravity loads, but also lateral loads due to earthquakes, wind, wave attack and vehicle impact loads, among others. Piles are subjected to destructive effects in the form of initial defects within the material or caused by fatigue or stress concentration. Especially, piles can suffer extreme damage and failure under earthquake loading and various the ground motions. Also, friction piles can be subjected to more destructive effects under the construction. As a result of destructive effects, cracks occur in the piles.

It is known that a crack in structure elements introduces a local flexibility, becomes more flexible and its dynamic and static behaviors will be changed. Cracks cause local flexibility and changes in structural stiffness. Therefore, understanding the mechanical behavior and the safe performance of cracked piles are importance in designs. After the construction, damage assessment and repair of the piles are very difficult in comparison with other structural elements. Therefore, the effect of the crack must be considered in the safe design of the piles.

In the literature, the vibration and dynamic behavior of the piles have been extensively studied. Valsangkar and Pradhanang [1] studied free vibration of partially supported piles with Winkler soil model. Xie and Vaziri [2] studied response of nonuniform piles to vertical vibrations. Lin and Al-Khaleefi [3] suidied torsional behavior of cracked reinforced

Concrete piles by using A finite element method. Khan and Pise [4] studied the dynamic behaviour of curved piles embedded in a homogeneous elastic half-space and subjected to forced harmonic vertical vibration. Lee et al. [5] investigated the natural frequencies and the mode shapes of the tapered piles embedded partially in the Winkler type foundations. Çatal [6] investigated free vibration of partially supported piles with the effects of bending moment, axial and shear force with the Winkler model. Filipich and Rosales [7] analysed the natural vibrations and critical loads of foundation beams embedded in a soil simulated with two elastic parameters through the Winkler–Pasternak model. Wang et al. [8] studied the dynamic response of pile groups embedded in a homogeneous poroelastic medium and subjected to vertical loading. Kim et al. [9] investigated vertical vibration analysis of soil-pile interaction systems considering the soil-pile interface behavior. Cairo et al. [10] analysed of vertically loaded pile groups under dynamic conditions. Yu-Jia et al. [11] nonlinear dynamical characteristics of piles under horizontal vibration based on continuum mechanics. Çatal [12] studied free vibration of semi-rigid connected and partially embedded piles with the effects of the bending moment, axial and shear force. Padron et al. [13] studied the dynamic analysis of piles and pile groups embedded in an elastic half-space with finite element metho- boundary element method coupling model. Dynamic behavior of group-piles in liquefied ground are investigated by Uzuoka et al. [14] using three-dimensional soil–water-coupled analysis with a soil–pile-building model. Masoumi and Degrande [15] investigated a numerical model for the prediction of free field vibrations due to vibratory and impact pile driving using a dynamic soil-structure interaction formulation. Tsai et al. [16] studied the screening effectiveness of circular piles in a row for a massless

square foundation subject to harmonic vertical loading with the three-dimensional boundary element method in frequency domain. Yeşilce and Çatal [17] investigated free vibration of piles embedded in soil having different modulus of subgrade reaction. Hu et al. [18] investiagted the nonlinear transverse vibration of piles under the assumption of that both the materials of pile and soil obey nonlinear elastic and linear viscoelastic constitutive relations. Yesilce and Çatal [19] investigated free vibration of semi-rigid connected piles embedded in elastic soil within Reddy-Bickford beam theory where the soil is modeled as Winkler model. Lu et al. [20] investigated the isolation of the vibration due to moving loads using pile rows embedded in a poroelastic half-space. Comodromos et al. [21] investigated effect of Cracking on the Response of Pile Test under Horizontal Loading. Bhattacharya et al. [22] investigated a unified buckling and free vibration analysis of pile-supported structures in seismically liquefiable soils that The pile–soil system is modelled as Euler–Bernoulli beam resting against an elastic support with axial load and a pile head mass with rotary inertia. The vertical dynamic response of an inhomogeneous viscoelastic pile embedded in layered soil subjected to axial loading has been investigated by Wang et al. [23]. Manna and Baidya [24] investigated dynamic response of cast-in-situ reinforced concrete piles subjected to strong vertical excitation. Yang and Pan [25] investigated the dynamical behavior of vertical vibration of an end-bearing pile in a saturated viscoelastic soil layer in the frequency domain using the Helmholtz decomposition and variable separation method. Dash et al. [26] investigated bending–buckling interaction as a failure mechanism of piles in liquefiable soils using numerical techniques. Haldar and Babu [27] investiagted the response of piles in liquefiable soil under seismic loads with the effects of soil, pile, and earthquake parameters on the two potential pile failure mechanisms, bending and buckling. Jian-hua et al. [28] investigated the dynamic response of a pile group embedded in a layered poroelastic half space subjected to axial harmonic loads. Zou et al. [29] investigated the influence of pile-soil-structure interaction on the vibration control of adjacent buildings with pile foundations. Jensen and Hoang [30] studied collapse mechanisms and strength prediction of reinforced concrete pile caps.

It is seen from literature that the vibration analysis of cracked piles has not been broadly investigated. A better understanding of the mechanism of how the crack effects change response of vibration of a pile is necessary, and is a prerequisite for further exploration and application of the cracked piles. Therefore, the distinctive feature of this study is the effect of location of crack, the depth of the crack on natural frequencies in detail.

Piles can be found in many different sizes and shapes in the engineering applications. Circular piles are the most used and preferred in the applications because of high energy absorbing capability and high buckling strength. Hence, understanding the mechanical behavior circular piles are very important.

In this study, free vibration analysis of an edge cracked piles with circular cross section is investigated. The soil that the pile partially embedded in is idealized by Winkler-Pasternak model. The governing differential equations of motion of the circular pile in free vibration are derived using Hamilton's principle. The pile–soil system is modeled as Euler–Bernoulli beam resting on Winkler-Pasternak foundation. The considered problem is solved by using finite element method. The cracked pile is modeled as an assembly of two sub-beams connected through a massless elastic rotational spring. In the study, the effects of the location of crack, the depth of the crack and the soil stiffness on the natural frequencies and mode shapes the piles are investigated in detail.

II.   THEORY AND FORMULATIONS

Consider a pile of length L, diameter D, containing an edge crack of depth a located at a distance L_1 from the bottom end, as shown in Figure 1. The soil–pile interaction is modeled as Winkler-Pasternak foundation with spring constant k_w and k_p. When the Pasternak foundation spring constant $k_{p=0}$, the soil–pile interaction model reduces to Winkler type. It is assumed that the crack is perpendicular to beam surface and always remains open.
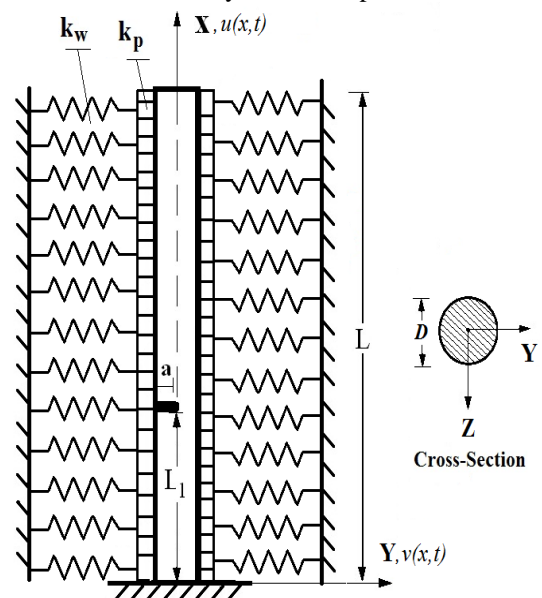

Figure 1 A circular pile with an open edge crack with Winkler-Pasternak soil model and cross-section.

2.1 GOVERNING EQUATION OF FREE VIBRATION OF INTACT PILES

The pile is modeled within the Euler-Bernoulli beam theory. According to the coordinate system *(X,Y,Z)* shown in figure 1, based on Euler-

Bernoulli beam theory, the axial and the transverse displacement field are expressed as

$$u(X,Y,t) = u_0(X,t) - Y \frac{\partial v_0(X,t)}{\partial X} \qquad (1)$$

$$v(X,Y,t) = v_0(X,t) \qquad (2)$$

Where u_0 and v_0 are the axial and the transverse displacements in the mid-plane, t indicates time. Using Eq. (1) and (2), the linear strain-displacement relation can be obtained:

$$\varepsilon_{XX} = \frac{\partial u}{\partial X} = \frac{\partial u_0(X,t)}{\partial X} - Y \frac{\partial^2 v_0(X,t)}{\partial X^2} \qquad (3)$$

According to Hooke's law, constitutive equations of the pile are as follows:

$$\sigma_{XX} = E\,\varepsilon_{XX} = E\left[\frac{\partial u_0(X,t)}{\partial X} - Y \frac{\partial^2 v_0(X,t)}{\partial X^2}\right] \qquad (4)$$

Where E is the Young's modulus of the pile, σ_{XX} and ε_{XX} are normal stresses and normal strains in the X direction, respectively. Based on Euler-Bernoulli beam theory, the elastic strain energy (V) and kinetic energy (T) of the pile with Winkler-Pasternak soil model is expressed as

$$V = \frac{1}{2}\int_0^L \int_A \sigma_{XX}\,\varepsilon_{XX}\,dA\,dX + \frac{1}{2}\int_0^L k_w\big(v(x,t)\big)^2 dX$$
$$+ \frac{1}{2}\int_0^L k_p\left(\frac{\partial v(x,t)}{\partial X}\right)^2 dX \qquad (5)$$

$$T = \frac{1}{2}\int_0^L \int_A \rho\left[\left(\frac{\partial u}{\partial t}\right)^2 + \left(\frac{\partial v}{\partial t}\right)^2\right] dA\,dx \qquad (6)$$

Where ρ is the mass density of the pile, with applying Hamilton's principle, the differential equations of motion are obtained as follows:

$$EA \frac{\partial^2 u_0}{\partial X^2} = \rho A \frac{\partial^2 u_0}{\partial t^2} \qquad (7)$$

$$-EI \frac{\partial^2}{\partial X^2}\left(\frac{\partial^2 v_0}{\partial X^2}\right) - k_w v_0 + k_p \frac{\partial^2 v_0}{\partial X^2}$$
$$= -\rho I \frac{\partial^2}{\partial t^2}\left(\frac{\partial v_0}{\partial X}\right) + \rho A \frac{\partial^2 v_0}{\partial t^2} \qquad (8)$$

Where I and A are the moment of inertia and the area of the cross-section, respectively.

2.2 FINITE ELEMENT FORMULATIONS

The displacement field of the finite element shown is expressed in terms of nodal displacements as follows:

$$u_0^{(e)}(X,t) = \varphi_1^{(v)}(X)\,u_1(t) + \varphi_2^{(v)}(X)\,u_2(t) \qquad (9)$$

$$v_0^{(e)}(X,t) = \varphi_1^{(v)}(X)\,v_1(t) + \varphi_2^{(v)}(X)\,\theta_1(t)$$
$$+ \varphi_3^{(v)}(X)\,v_2(t) + \varphi_4^{(v)}(X)\,\theta_2(t) \qquad (10)$$

where u_i, v_i and θ_i are axial displacements, transverse displacements and slopes at the two end nodes of the pile element, respectively. $\varphi_i^{(v)}$ and $\varphi_i^{(v)}$ are interpolation functions for axial and transverse degrees of freedom, respectively, which are given in Appendix. Two-node pile element shown in Figure 2.
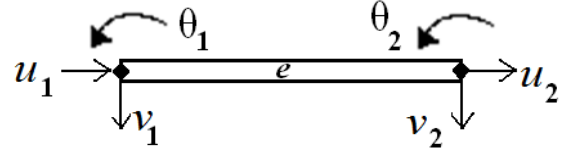

Figure 2 A two-node pile element.

With using the standard procedure of the Galerkin finite element method, the stiffness matrix and the mass matrix are obtained according to Eqs. (7) and (8). The equation of motion as follows:

$$[K]\{q\} + [M]\{\ddot{q}\} = 0 \qquad (11)$$

where $[K]$ is the stiffness matrix and $[M]$ is the mass matrix. $\{q\}$ is nodal displacement vector which as follows

$$\{q\} = \{u, v, \theta\}^T \qquad (12)$$

The stiffness matrix $[K]$ can be expressed as a sum of three submatrices as shown below:

$$[K] = \big[K_{(b)}\big] + \big[K_{(w)}\big] + \big[K_{(p)}\big] \qquad (13)$$

Where $\big[K_{(b)}\big]$, $\big[K_{(w)}\big]$ and $\big[K_{(p)}\big]$ are pile stiffness matrix, Winkler foundation stiffness matrix and Pasternak foundation stiffness matrix, respectively. Explicit forms of $[K]$ are given in Appendix. The mass matrix $[M]$ can be expressed as a sum of four sub-matrices as shown below:

$$[M] = [M_u] + [M_v] + [M_\theta] \qquad (14)$$

Where $[M_u]$, $[M_v]$ and $[M_\theta]$ are the contribution of u, v and θ degree of freedom to the mass matrix, respectively. Explicit forms of $[M]$ are given in Appendix.

2.3. CRACK MODELING

The cracked pile is modeled as an assembly of two sub-beams connected through a massless elastic rotational spring shown in figure 3.
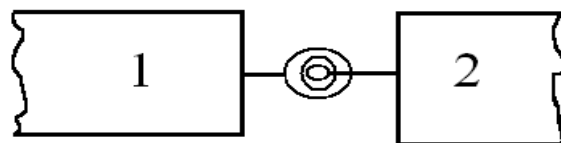

Figure 3 Rotational Spring Model.

The additional strain energy due to the existence of the crack can be expressed as

The bending stiffness of the cracked section k_T is related to the flexibility G by

$$k_T = \frac{1}{G} \qquad (15)$$

Cracked section's flexibility G can be derived from Broek's approximation [31]:

$$\frac{(1-v^2)K_I^2}{E} = \frac{M^2}{2}\frac{dG}{da} \qquad (16)$$

where M is the bending moment at the cracked section, k_I is the stress intensity factor (SIF) under mode I bending load and is a function of the geometry and the loading properties as well. v indicates Poisson's ratio. For circular cross section, the stress intensity factor for k_I a single edge cracked beam specimen under pure bending M can be written as follow (Tada et al. [32])

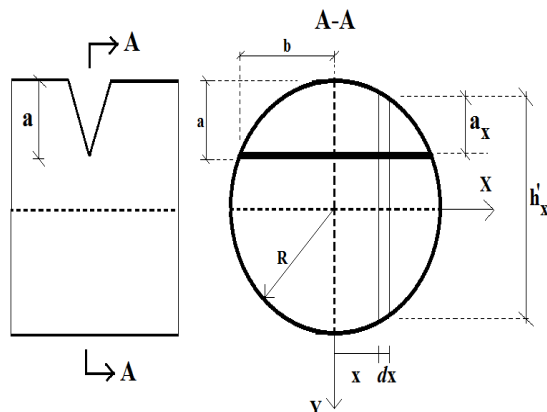$$K_I = \frac{4M}{\pi R^4}\frac{h_x'}{2}\sqrt{\pi a}\, F(a/h_x') \qquad (17)$$

Where

$$F(a/h_x') = \sqrt{\frac{2h_x'}{\pi a} tg\left(\frac{\pi a}{2h_x'}\right)}\ \frac{0.923+0.199\left(1-\sin\left(\frac{\pi a}{2h_x'}\right)\right)^4}{\cos\left(\frac{\pi a}{2h_x'}\right)} \qquad (18)$$

Where a is crack of depth and h_x' is the height of the strip, is shown Fig. 4, and written as

$$h_x' = 2\sqrt{R^2 - x^2} \qquad (19)$$

where R is the radius of the cross section of the beam.

Figure 4 The geometry of the cracked circular cross section.

After substituting Eq. (17) into Eq. (16) and by integrating Eq. (16), the flexibility coefficient of the crack section G is obtained as

$$G = \frac{32(1-v^2)}{E\pi R^8}\int_{-b}^{b}\int_{0}^{a_x} y(R^2 - x^2)F^2\,(a/h_x')\,dx\,dy \qquad (20)$$

where b and a_X are the boundary of the strip and the local crack depth respectively, are shown in Fig. 4, respectively, and written as

$$b = \sqrt{R^2 - (R-a)^2} \qquad (21)$$

$$a_X = \sqrt{R^2 - x^2} - (R-a) \qquad (22)$$

The spring connects the adjacent left and right elements and couples the slopes of the two pile elements at the crack location. In the massless spring model, the compatibility conditions enforce the continuities of the axial displacement, transverse deflection, axial force and bending moment across the crack at the cracked section $(X=L_I)$, that is,

$$u_1 = u_2,\ v_1 = v_2,\quad N_1 = N_2,\quad M_1 = M_2, \qquad (23)$$

The discontinuity in the slope is as follows:

$$k_T\left(\frac{dv_1}{dX} - \frac{dv_2}{dX}\right) = k_T(\theta_1 - \theta_2) = M_1 \qquad (24)$$

Based on the massless spring model, the stiffness matrix of the cracked section as follows:

$$[K]_{(Cr)} = \begin{bmatrix} 1/G & -1/G \\ -1/G & 1/G \end{bmatrix} = \begin{bmatrix} k_T & -k_T \\ -k_T & k_T \end{bmatrix} \qquad (25)$$

The stiffness matrix of the cracked section is written according to the displacement vector:

$$\{q\}_{(cr)} = \{\theta_1,\ \theta_2\}^T \qquad (26)$$

Where θ_1 and θ_1 are the angles of the cracked section. With adding crack model, the equations of motion for the finite element and by use of usual assemblage procedure the following system of equations of motion for the whole system can be obtained as follows:

$$([K] + [K]_{(Cr)})\,\{q\} + [M]\{\ddot{q}\} = 0 \qquad (27)$$

If the global nodal displacement vector $\{q\}$ is assumed to be harmonic in time with circular frequency ω, i.e $\{q\} = \{\hat{q}\}e^{i\omega t}$ becomes, after imposing the appropriate end conditions, an eigenvalue problem of the form:

$$([K] + [K]_{(Cr)} - \omega^2[M])\{\hat{q}\} = 0 \qquad (28)$$

Where $\{q\}$ is a vector of displacement amplitudes of the vibration. The dimensionless quantities can be expressed as

$$\bar{\omega} = \omega L^2 \sqrt{\frac{\rho A}{EI}}, \ \bar{k}_w = \frac{k_w L^4}{EI}, \ \bar{k}_p = \frac{k_p L^2}{EI}$$

$$\bar{X} = \frac{X}{L}, \ \bar{Y} = \frac{X}{D} \qquad (29)$$

Where $\bar{\omega}$ is the dimensionless frequency, $\bar{k}_w$ is the dimensionless Winkler parameter, $\bar{k}_p$ is the dimensionless Pasternak parameter,

III. NUMERICAL RESULTS

In the numerical examples, the natural frequencies and the mode shapes of the piles are calculated and presented in figures for various the effects of the location of crack, the depth of the crack and foundation stiffness. In the numerical examples, the physical properties of the pile are Young's modulus E=206 *GPa*, Poisson's ratio *v*=0,3 and mass density ρ=7800 *kg/m³*. The geometrical properties of the pile are length L=30*m* and the diameter D= 1 m. In the numerical calculations, the number of finite elements is taken as n =100 and five-point Gauss integration rule is used.

In figure 5, the effect of crack locations (L_1/L) on the dimensionless fundamental frequency $\bar{\omega}_1$ of edge cracked piles is shown for different crack depth ratios (a/D=0.1, 0.2, 0.35) for $\bar{k}_w = 10$ and $\bar{k}_p = 3$.
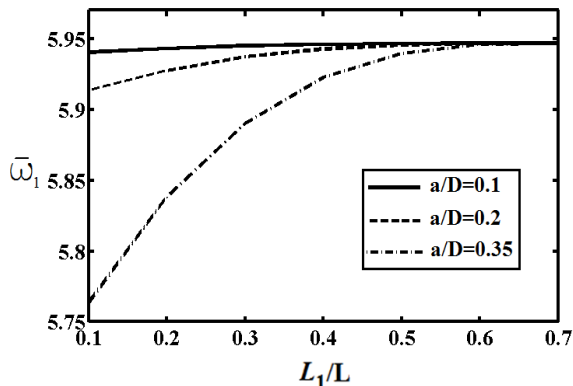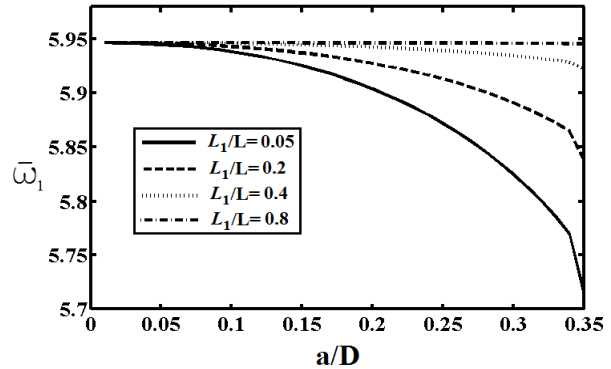

Figure 5 The effect of crack locations (L_1/L) on the dimensionless fundamental frequency $\bar{\omega}_1$ for different crack depth ratios (a/D=0.1, 0.2, 0.35).

Fig. 5 shows that the crack locations get closer to the bottom end, the fundamental frequency decreases. This is because the crack at the fixed end (bottom end) has a most severe effect in the pile. So, the crack locations get closer to the bottom end, the pile gets more flexible. Also, It is seen Figure 5 that the crack locations get closer to the top end (lower values of L_1/L), the differences of the crack depth ratio *a/h* decrease seriously and the cracked pile seems like intact pile. It is seen from Fig. 5 that almost all of the curves have horizontal asymptotes approximately after the crack location $L_1/L=0.6$.

In figure 6, the effect of crack depth ratio a/D on the dimensionless fundamental frequency $\bar{\omega}_1$ of edge cracked pile is shown for different crack locations (L_1/L=0.05, 0.2, 0.4, 0.8) for $\bar{k}_w = 10$ and $\bar{k}_p = 3$.
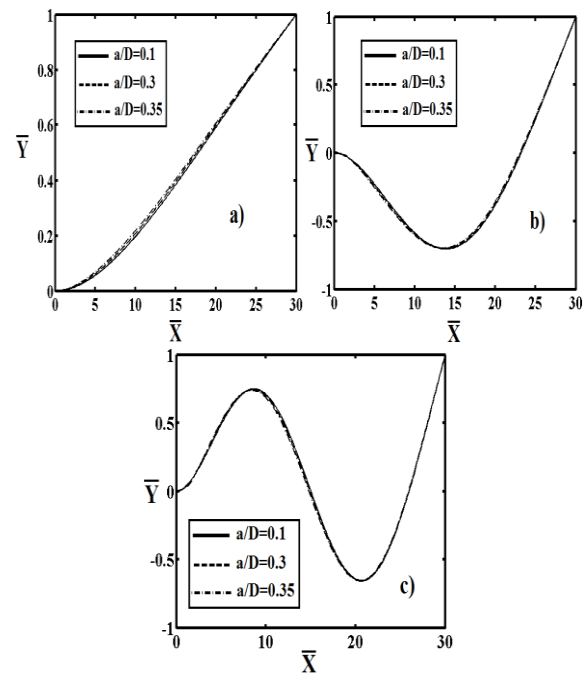

Figure 6 The effect of crack depth ratio a/D on the dimensionless fundamental frequency $\bar{\omega}_1$ for different crack locations (L_1/L=0.05, 0.2, 0.4, 0.8).

It is observed from Fig. 6 that with increase in the crack depth ratio (a/D), the fundamental frequency decreases seriously. This is because increasing the crack depth ratio (a/D), the pile becomes flexible. Also, It is seen Figure 6 that there is a significant difference of the crack locations in the high values of crack depth ratios a/D.
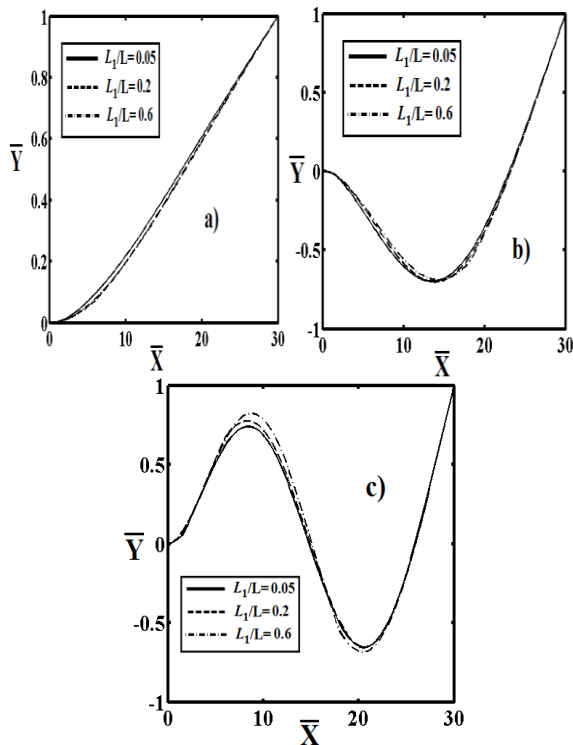
In Fig. 7, the effect of crack depth ratio (a/D) on the first, second and third normalized vibration mode shapes is shown for L_1/L=0.05, $\bar{k}_w = 10$, $\bar{k}_p = 3$.

In fig. 8, the effect of the crack location L_1/L on the first, second and third normalized vibration mode shapes is shown for a/D=0.35, $\bar{k}_w = 10$ and $\bar{k}_p = 3$.

Figure 7 The effect the crack depth ratio a/D on the a) first, b) second and c) third normalized vibration mode shapes.
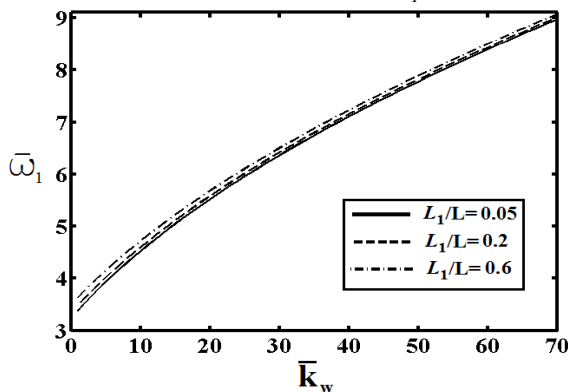
Figure 8 The effect the crack location L_1/L on the a) first, b) second and c) third normalized vibration mode shapes.

It is seen from Fig. 7 and Fig. 8 that the crack depth ratio a/D and the crack location L_1/L play important role on the vibration mode shapes.

In figure 9, the effect of the dimensionless Winkler parameter $\bar{k}_w$ on the dimensionless fundamental frequency $\bar{\omega}_1$ of edge cracked pile (a/D =0,35, $\bar{k}_p$=0) is shown for different crack location L_1/L.
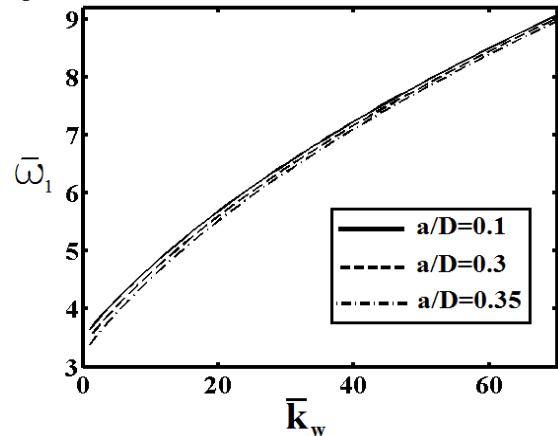

Figure 9 The effect the dimensionless Winkler parameter $\bar{k}_w$ on the dimensionless fundamental frequency $\bar{\omega}_1$ for different crack location L_1/L.

It is seen from Fig. 9 the Winkler parameters $\bar{k}_w$ play important role on the fundamental frequency. With increase in the dimensionless Winkler parameter $\bar{k}_w$, the fundamental frequency increases. This is because, the dimensionless Winkler parameter $\bar{k}_w$ increase, the pile gets more stiffer. Also, it is

observed fig. 9 that the differences of the crack locations (L_1/L) decrease with increase in the Winkler parameter $\bar{k}_w$.
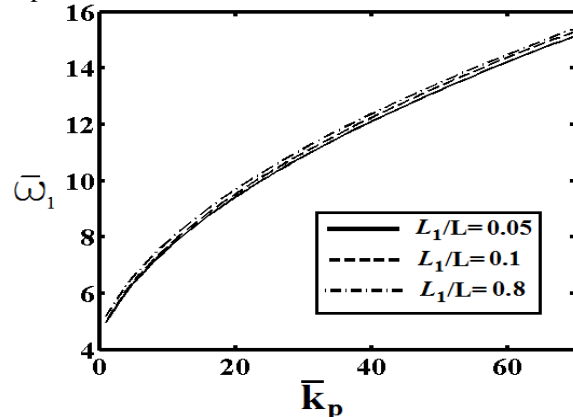
In figure 10, the effect of the dimensionless Winkler parameter $\bar{k}_w$ on the dimensionless fundamental frequency $\bar{\omega}_1$ of edge cracked pile (L_1/L= 0.05, $\bar{k}_p = 0$) is shown for different crack depth ratios a/D.
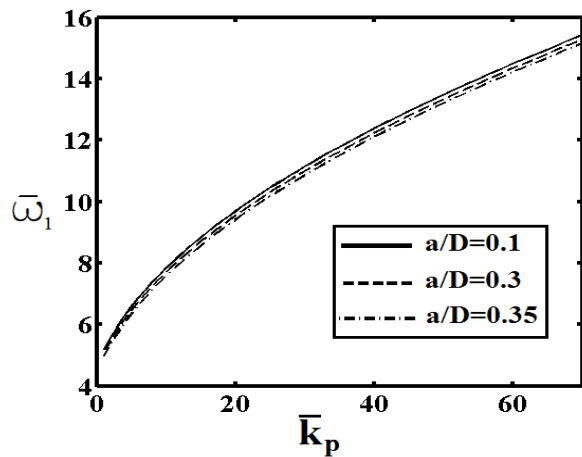

Figure 10 The effect the dimensionless Winkler parameter $\bar{k}_w$ on the dimensionless fundamental frequency $\bar{\omega}_1$ for different the crack depth ratio a/D.

It is observed from Fig. 10 that with the increasing the value of the dimensionless Winkler parameter $\bar{k}_w$, the differences of the crack depth ratio (a/D) decrease. With increase in the soil stiffness parameter, the effects of the crack reduce.

In figure 11, the effect of the dimensionless Pasternak parameter $\bar{k}_p$ on the dimensionless fundamental frequency $\bar{\omega}_1$ of edge cracked piles ($a/D=0.35$, $\bar{k}_w = 10$) is shown for different the crack location L_1/L. In Figure 12, the effect of the dimensionless Pasternak parameter $\bar{k}_p$ on the dimensionless fundamental frequency $\bar{\omega}_1$ of edge cracked piles ($L_1/L=0.05$, $\bar{k}_w = 10$) is shown for different the crack depth ratio a/D.

Figure 11 The effect the dimensionless Pasternak parameter $\bar{k}_p$ on the dimensionless fundamental frequency $\bar{\omega}_1$ for different the crack location L_1/L.

Figure 12 The effect the dimensionless Pasternak parameter $\overline{k}_p$ on the dimensionless fundamental frequency $\overline{\omega}_1$ for various the crack depth ratio *a/D*.

It is seen from Fig. 11 and Fig. 12 that with increase in the dimensionless Pasternak parameter $\overline{k}_p$, the fundamental frequency increases. This is because increasing the Pasternak parameter $\overline{k}_p$, the pile becomes more stiffer. Also, it is observed from the results, the effect of Pasternak parameter $\overline{k}_p$ on the dimensionless fundamental frequency is less than Winkler parameter $\overline{k}_w$.

IV. CONCLUSIONS

Free vibration analysis of an edge cracked piles with circular cross section is investigated. The soil medium is modeled as Winkler-Pasternak elastic foundation approach. The differential equations of motion are obtained by using Hamilton's principle. The pile–soil system is modeled as Euler–Bernoulli beam resting on Winkler-Pasternak foundation. The considered problem is solved by using finite element method. The cracked beam is modeled as an assembly of two sub-beams connected through a massless elastic rotational spring. The influences of the location of crack, the depth of the crack and foundation stiffness on the natural frequencies and the mode shapes of the piles are examined in detail.

It is observed from the investigations that the crack locations and the crack depth have a great influence on the vibration characteristics of the piles. There are significant differences of the mechanical behaviour for the cracked and intact piles. Also, it is seen from the investigations that, the stiffness parameter of soil is very effective for reducing disadvantage of cracks. The effect of the crack on the piles must be considered at the design stage.

APPENDİX

The interpolation functions for axial degrees of freedom are

$$\varphi^{(U)}(X) = \left[\varphi_1^{(U)}(X) \quad \varphi_2^{(U)}(X)\right]^T, \qquad (A1)$$

Where

$$\varphi_1^{(U)}(X) = \left(-\frac{X}{L_e} + 1\right), \qquad (A2)$$

$$\varphi_2^{(U)}(X) = \left(\frac{X}{L_e}\right), \qquad (A3)$$

The interpolation functions for transverse degrees of freedom are

$$\varphi^{(V)}(X) = \left[\varphi_1^{(V)}(X) \quad \varphi_2^{(V)}(X) \quad \varphi_3^{(V)}(X) \quad \varphi_4^{(V)}(X)\right]^T \text{(A4)}$$

Where

$$\varphi_1^{(V)}(X) = \left(1 - \frac{3X^2}{L_e^2} + \frac{2X^3}{L_e^3}\right), \qquad (A5)$$

$$\varphi_2^{(V)}(X) = \left(-X + \frac{2X^2}{L_e} - \frac{X^3}{L_e^2}\right), \qquad (A6)$$

$$\varphi_3^{(V)}(X) = \left(\frac{3X^2}{L_e^2} - \frac{2X^3}{L_e^3}\right), \qquad (A7)$$

$$\varphi_4^{(V)}(X) = \left(\frac{X^2}{L_e} - \frac{X^3}{L_e^2}\right), \qquad (A8)$$

Where L_e indicates the length of the finite pile element. The components of the stiffness matrix $[K]$: the pile stiffness matrix $[K_{(b)}]$, Winkler foundation stiffness matrix $[K_{(w)}]$ and Pasternak foundation stiffness matrix $[K_{(p)}]$ are as follows

$$[K_{(b)}] = \begin{bmatrix} [K_{(b)}^A] & [0] \\ [0] & [K_{(b)}^D] \end{bmatrix}, \qquad (A9)$$

Where

$$[K_{(b)}^A] = \int_0^{L_e} EA \left[\frac{d\varphi^{(U)}}{dX}\right]^T \left[\frac{d\varphi^{(U)}}{dX}\right] dX, \qquad (A10)$$

$$[K_{(b)}^D] = \int_0^{L_e} EI \left[\frac{d^2\varphi^{(V)}}{dX^2}\right]^T \left[\frac{d^2\varphi^{(V)}}{dX^2}\right] dX, \qquad (A11)$$

$$[K_w] = \int_0^{L_e} k_w \left[\varphi^{(V)}\right]^T \left[\varphi^{(V)}\right] dX, \qquad (A12)$$

$$[K_p] = \int_0^{L_e} k_p \left[\frac{d\varphi^{(V)}}{dX}\right]^T \left[\frac{d\varphi^{(V)}}{dX}\right] dX, \qquad (A13)$$

The components of the mass matrix $[M]$: $[M_u]$, $[M_v]$ and $[M_\theta]$ $[M_q]$ are as follows

$$[M_u] = \int_0^{L_e} \rho A \left[\varphi^{(U)}\right]^T \left[\varphi^{(U)}\right] dX \qquad (A14)$$

$$[M_V] = \int_0^{L_e} \rho A \left[\varphi^{(V)}\right]^T \left[\varphi^{(V)}\right] dX \qquad (A15)$$

$$[M_\theta] = \int_0^{L_e} \rho I \left[\frac{d\varphi^{(V)}}{dX}\right]^T \left[\frac{d\varphi^{(V)}}{dX}\right] dX \qquad \text{(A16)}$$

REFERENCES

[1] A.J. Valsangkar, R.B. Pradhanang, Free Vibration of Partially Supported Piles, *Journal of Engineering Mechanic,s 113(8),* 1987, 1244-1247.

[2] J. Xie, H.H. Vaziri, Vertical Vibration of Nonuniform Piles, *Journal of Engineering Mechanics, 117(5),* 1991, 1105-1118.

[3] S-S.Lin, A.L.Al-Khaleefi, Torsional behavior of cracked reinforced concrete piles in sand, *Journal of the Chinese Institute of Engineers, 19(6),* 1996, 689-696.

[4] A.K. Khan, P.J. Pise, Dynamic behaviour of curved piles, *Computers & Structures, 65(6),* 1997, 795-807.

[5] B.K. Lee, J.S. Jeong, L.G. Fan, T.K. Jin, Free vibrations of tapered piles embedded partially in Winkler type foundations, *KSCE Journal of Civil Engineering, 3(2),* 1999, 195-203.

[6] H.H. Çatal, Free vibration of partially supported piles with the effects of bending moment, axial and shear force, *Engineering Structures, 24(12)* , 2002, 1615–1622.

[7] C.P. Filipich, M.B. Rosales, A further study about the behaviour of foundation piles and beams in a Winkler–Pasternak soil, *International Journal of Mechanical Sciences, 44(1),* 2002, 21-36.

[8] J.H. Wang, X.L. Zhou, J.F. Lu, Dynamic response of pile groups embedded in a poroelastic medium, *Soil Dynamics and Earthquake Engineering, 2(3),* 2003, 53-60.

[9] M.K. Kim, J.S. Lee, M.K. Kim, Vertical vibration analysis of soil-pile interaction systems considering the soil-pile interface behavior, *KSCE Journal of Civil Engineering, 8(2),* 2004, 221-226.

[10] R. Cairo, E. Conte, G. Dente, Analysis of pile groups under vertical harmonic vibration, *Computers and Geotechnics, 32(7),* 2005, 545–554.

[11] H.Yu-Jia, C.Chang-Jun, Y.Xiao, Nonlinear dynamical characteristics of piles under horizontal vibration, *Applied Mathematics and Mechanics, 26(6),* 2005, 700-708.

[12] H.H.Çatal, Free vibration of semi-rigid connected and partially embedded piles with the effects of the bending moment, axial and shear force, *Engineering Structures, 28(14),* 2006, 1911–1918.

[13] L.A. Padrón, J.J. Aznárez, O. Maeso, BEM–FEM coupling model for the dynamic analysis of piles and pile groups, *Engineering Analysis with Boundary Elements, 3(6)1,* 2007, 473-484.

[14] R. Uzuoka, N. Sento, M. Kazama, F. Zhang, A.Yashima, F.Oka, Three-dimensional numerical simulation of earthquake damage to group-piles in a liquefied ground, *Soil Dynamics and Earthquake Engineering ,27(5),* 2007, 395-413.

[15] H.R. Masoumi, G.Degrande, Numerical modeling of free field vibrations due to pile driving using a dynamic soil-structure interaction formulation, *Journal of Computational and Applied Mathematics, 215(2),* 2008, 503–511.

[16] P-H Tsai, Z-Y Feng, T-L Jen, Three-dimensional analysis of the screening effectiveness of hollow pile barriers for foundation-induced vertical vibration, *Computers and Geotechnics, 35(3),* 2008, 489-499.

[17] Y. Yesilce, H. H. Çatal, Free vibration of piles embedded in soil having different modulus of subgrade reaction, *Applied Mathematical Modelling, 32(5),* 2008, 899-900.

[18] C-L. Hu, C-J. Cheng, Z-X. Chen, Nonlinear transverse free vibrations of piles, *Journal of Sound and Vibration, 317(3),* 2008, 937-954.

[19] Y. Yesilce, H. H. Çatal, Free vibration of semi-rigid connected Reddy-Bickford piles embedded in elastic soil, *Sadhana, 33(6), 2008,* 781-801.

[20] J-F. Lu, B. Xu, J-H. Wang, Numerical analysis of isolation of the vibration due to moving loads using pile rows, *Journal of Sound and Vibration, 319(3-5),* 2009, 940-962.

[21] E. M. Comodromos, M. C. Papadopoulou, I, K. Rentzeperis, Effect of Cracking on the Response of Pile Test under Horizontal Loading, *Journal of Geotechnical and Geoenvironmental Engineering, 135(9),* 2009, 1275-1284.

[22] S. Bhattacharya, S. Adhikari, N.A. Alexander, A simplified method for unified buckling and free vibration analysis of pile-supported structures in seismically liquefiable soils, *Soil Dynamics and Earthquake Engineering, 29(8),* 2009, 1220-1235.

[23] K. Wang, W. Wu, Z. Zhang, C. J. Leo, Vertical dynamic response of an inhomogeneous viscoelastic pile. *Computers and Geotechnics, 37(4),* 2010, 536-544.

[24] B. Manna, D.K. Baidya, Dynamic nonlinear response of pile foundations under vertical vibration—Theory versus experiment, *Soil Dynamics and Earthquake Engineering, 30(6),* 2010, 456-469.

[25] X. Yang, Y. Pan, Axisymmetrical analytical solution for vertical vibration of end-bearing pile in saturated viscoelastic soil layer,

Applied Mathematics and Mechanics, 31(2), 2010, 193-204.

[26] S. R. Dash, S. Bhattacharya, A. Blakeborough, Bending–buckling interaction as a failure mechanism of piles in liquefiable soils, *Soil Dynamics and Earthquake Engineering, 30(1-2),* 2010, 32-39.

[27] S. Haldar, G. L. S. Babu, Failure Mechanisms of Pile Foundations in Liquefiable Soil: Parametric Study, *International Journal of Geomechanics, 10(2)*, 2010, 74-84.

[28] L. Jian-hua, X. Man-qing, X. Bin, F. Ming-fu, The Vibration of Pile Groups Embedded in a Layered Poroelastic half Space Subjected to Harmonic Axial Loads by using Integral Equations Method, *Procedia Engineering, 28(2012)*, 2012, 8-11.

[29] L. Zou, K. Huang, L. Wang, J. Butterworth, X. Ma, Vibration control of adjacent buildings considering pile-soil-structure interaction, *Journal of Vibration and Control, 18(5)*, 2012, 684-695.

[30] U.G. Jensen, L.C. Hoang, Collapse mechanisms and strength prediction of reinforced concrete pile caps, *Engineering Structures, 35*, 2012, 203-214.

[31] D. Broek, *Elementary engineering fracture mechanics* (Martinus Nijhoff Publishers, Dordrecht, 1986).

[32] H. Tada, P.C. Paris and G.R. Irwin, *The Stress Analysis of Cracks Handbook* (Paris Production Incorporated and Del Research Corporation, 1985).